Modeling of an All-Optical Raman Modulator in Silicon-on-Insulator Technology

F. De Leonardis and V. M. N. Passaro °

Dipartimento di Ingegneria dell'Ambiente e per lo Sviluppo Sostenibile, Politecnico di Bari, viale del Turismo n. 8, 74100 Taranto, Italy

° Photonics Research Group, Dipartimento di Elettrotecnica ed Elettronica, Politecnico di Bari, via Edoardo Orabona n. 4, 70125 Bari, Italy

The high Raman gain and small mode area in Silicon-on-Insulator (SOI) rib waveguides make the Stimulated Raman Scattering observable over the millimetre-scale interaction length, usually encountered in integrated optical devices. In this paper, we propose the theoretical study and simulation of a novel all-optical intensity modulator based on Raman effect in SOI rib waveguide, as an all-optical signal processing device highly suitable for high speed systems in order to avoid the usual bottlenecks associated with electrical-to-optical and optical-to-electrical signal conversion. Some numerical examples are given to show the device principle of operation.

Modulator architecture

The architecture of the integrated all-optical intensity modulator is shown in Fig. 1.

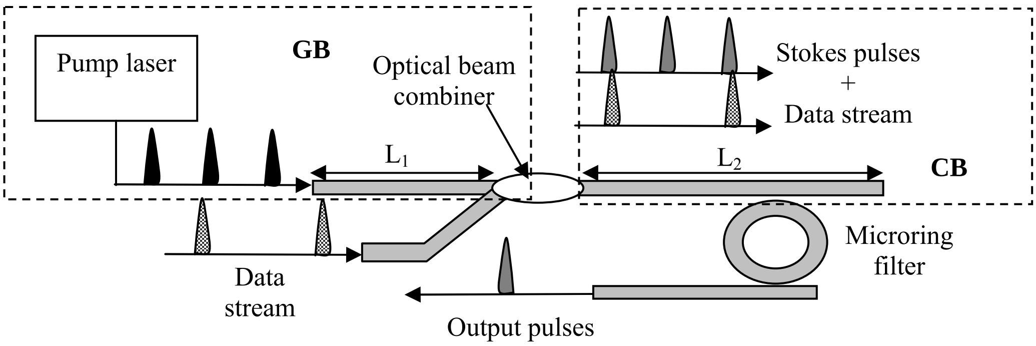

Fig. 1. Architecture of the all-optical Raman intensity modulator.

Two different blocks can be recognized, the generation block (GB), where a pump signal is launched into the SOI rib waveguide travelling over a length L_1, and a cancellation block (CB). If the pump power is large enough, a Stokes pulse is generated via Stimulated Raman Scattering (SRS). When a data stream is introduced at the optical beam combiner, the power transfer from the data to the Stokes pulses occurs if the pulses are quasi velocity-matched. Since the power transfer occurs if a space-time overlap between data and Stokes pulses is verified, the Stokes pulse will erase only the matched data pulse, selected in the cancellation block (CB) of length L_2. Finally, a selective Bragg grating or microring filter is used to extract at the output only the modulated data signal. Although this principle of operation is similar to that already presented in literature [1], here it is investigated in a totally integrated optical silicon architecture.

Since the cancellation is due to an all-optical power transfer mechanism between different optical pulses, the usual hypothesis of quasi-continuous wave operation cannot be used. In fact, it applies for experimental investigation in SOI waveguides where the pump pulses have a full wave half maximum time width $T_{FWHM} \geq$ 1 ns, the walk-off length L_w generally exceeding the waveguide length L. However, for ultrashort pulses with $T_{FWHM} < 10$ ps, typically it holds $L_w \leq L$. SRS is then limited by the group-velocity mismatch and occurs only over distances $z \sim L_w$ even if the actual waveguide length L is considerable larger than L_w. At the same time, the nonlinear effects such as self phase modulation (SPM) and cross phase modulation (XPM) can become important and affect the evolution of both pump and Raman pulses. Thus, in this situation the time derivative cannot be neglected and appropriate numerical techniques are necessary to solve the partial differential equation system governing the mutual interaction among Stokes, pump and data pulses..

Modeling and numerical results

The goal of the proposed modeling is to include all nonlinear effects involved in the SOI device in a general and self-consistent formalism. In particular, in both GB and CB we have considered Raman effect (generation of the fundamental, first and second order Stokes waves), walk-off effect, SPM and XPM induced by Kerr effect, two photon absorption (TPA), plasma dispersion and free carrier absorption (FCA) induced by TPA. It is worth to note that the TPA effect is generated only by the pump pulse in GB, while TPA is produced in CB by the combination of the residual pump, data stream pulse and fundamental Stokes wave. Therefore, the model is constituted by a rate equation for the time dynamics of TPA generated free carriers and by a system of partial differential equations in time and space domains, written in GB section as:

$$
\begin{cases}
\dfrac{\partial A_p}{\partial z} + \beta_{1p}\dfrac{\partial A_p}{\partial t} + j\dfrac{1}{2}\beta_{2p}\dfrac{\partial^2 A_p}{\partial t^2} = -\dfrac{\left(\alpha_p^{(prop)} + \alpha_p^{(FCA)}\right)}{2}A_p - 0.5\beta^{(TPA)} f_{p,p}\left|A_p\right|^2 A_p + j\gamma_{p,p}\left|A_p\right|^2 A_p + \\
+ j2\gamma_{p,s0}\left|A_{s0}\right|^2 A_p + j\dfrac{2\pi}{\lambda_p}\Delta n_p A_p - \dfrac{1}{2}g_R\dfrac{\omega_p}{\omega_{s0}} f_{p,s0}\left|A_{s0}\right|^2 A_p \\
\dfrac{\partial A_{s0}}{\partial z} + \beta_{1,s0}\dfrac{\partial A_{s0}}{\partial t} + j\dfrac{1}{2}\beta_{2,s0}\dfrac{\partial^2 A_{s0}}{\partial t^2} = -\dfrac{\alpha_{s0}^{(prop)}}{2}A_{s0} - \dfrac{1}{2}\alpha_{s0}^{(FCA)}A_{s0} - \beta^{(TPA)} f_{s0,p}\left|A_p\right|^2 A_{s0} + j2\gamma_{s0,p}\left|A_p\right|^2 A_{s0} + j\gamma_{s0,s0}\left|A_{s0}\right|^2 A_{s0} \\
+ j\dfrac{2\pi}{\lambda_{s0}}\Delta n_{s0}A_{s0} + \dfrac{1}{2}g_{R,s0} f_{s0,p}\left|A_p\right|^2 A_{s0} - \dfrac{1}{2}g_{R,s0} f_{s0,s1}\left|A_{s1}\right|^2 A_{s0} \\
\dfrac{\partial A_{s1}}{\partial z} + \beta_{1,s1}\dfrac{\partial A_{s1}}{\partial t} + j\dfrac{1}{2}\beta_{2,s1}\dfrac{\partial^2 A_{s1}}{\partial t^2} = -\dfrac{\alpha_{s1}^{(prop)}}{2}A_{s1} - \dfrac{1}{2}\alpha_{s1}^{(FCA)}A_{s1} - \beta^{(TPA)} f_{s1,p}\left|A_p\right|^2 A_{s1} + j2\gamma_{s1,s0}\left|A_{s0}\right|^2 A_{s1} + j2\gamma_{s1,p}\left|A_p\right|^2 A_{s1} \\
+ j\gamma_{s1,s1}\left|A_{s1}\right|^2 A_{s1} + j\dfrac{2\pi}{\lambda_{s1}}\Delta n_{s1}A_{s1} + \dfrac{1}{2}g_{R,s1} f_{s1,s0}\left|A_{s0}\right|^2 A_{s1} - \dfrac{1}{2}g_{R,s1} f_{s1,s2}\left|A_{s2}\right|^2 A_{s0} \\
\dfrac{\partial A_{s2}}{\partial z} + \beta_{1,s2}\dfrac{\partial A_{s2}}{\partial t} + j\dfrac{1}{2}\beta_{2,s2}\dfrac{\partial^2 A_{s2}}{\partial t^2} = -\dfrac{\left(\alpha_{s2}^{(pt)} + \alpha_{s2}^{(FCA)}\right)}{2}A_{s2} - \beta^{(TPA)} f_{s2,p}\left|A_p\right|^2 A_{s2} + j2\gamma_{s2,s1}\left|A_{s1}\right|^2 A_{s2} + j\gamma_{s2,s2}\left|A_{s2}\right|^2 A_{s2} + \\
+ j2\gamma_{s2,p}\left|A_p\right|^2 A_{s2} + j2\gamma_{s2,s0}\left|A_{s0}\right|^2 A_{s2} + j\dfrac{2\pi}{\lambda_{s2}}\Delta n_{s2}A_{s2} + \dfrac{1}{2}g_{R,s2} f_{s2,s1}\left|A_{s1}\right|^2 A_{s2} \\
\dfrac{\partial A_{s2}}{\partial t} + j\dfrac{1}{2}\beta_{2,s2}\dfrac{\partial^2 A_{s2}}{\partial t^2} = -\dfrac{\left(\alpha_{s2}^{(pt)} + \alpha_{s2}^{(FCA)}\right)}{2}A_{s2} - \beta^{(TPA)} f_{s2,p}\left|A_p\right|^2 A_{s2} + j2\gamma_{s2,s1}\left|A_{s1}\right|^2 A_{s2} + j\gamma_{s2,s2}\left|A_{s2}\right|^2 A_{s2} + \\
+ j2\gamma_{s2,p}\left|A_p\right|^2 A_{s2} + j2\gamma_{s2,s0}\left|A_{s0}\right|^2 A_{s2} + j\dfrac{2\pi}{\lambda_{s2}}\Delta n_{s2}A_{s2} + \dfrac{1}{2}g_{R,s2} f_{s2,s1}\left|A_{s1}\right|^2 A_{s2}
\end{cases}
$$

Moreover, it is clear that the model involves five partial differential equations in CB section, for residual pump, data pulse, fundamental Stokes pulse, first and second order Stokes waves. They are similar to the previous ones and are not reported here.

The main design criteria selected for our device have been absence of any birefringence in nano-scale SOI rib waveguide for the fundamental Stokes wave and no excitation of higher order Stokes waves in both GB and CB sections. As an example, by assuming a pump pulse at λ_p = 1.4332 μm, the condition of free polarization for the fundamental Stokes wave (λ_{s0} = 1.5487 μm) can be obtained using a SOI waveguide with a rib total height H = 500 nm, a slab height H_s =150 nm and rib width W = 396 nm [2]. Other numerical parameters were $T_{FWHM} = 100\,\text{ps}$ for both pump and data pulses (1.67 Gb/s pulse rate in this case), and Raman gain $g_R = 10.5$ cm/GW. Then, the excitation of higher order Stokes waves in GB is avoided assuming a peak pump power $P_0 = 1.5$ W and a waveguide length $L_1 = 10$ mm. Fig. 2 shows the time-space evolution of data pulse in CB, with the cancellation by the fundamental Stokes pulse (see also Fig. 3).

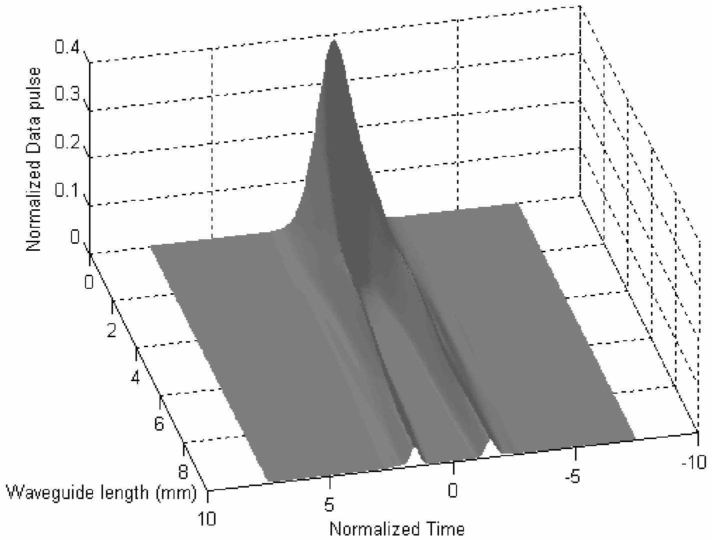

Fig. 2. Time-space evolution of data pulse in CB section.

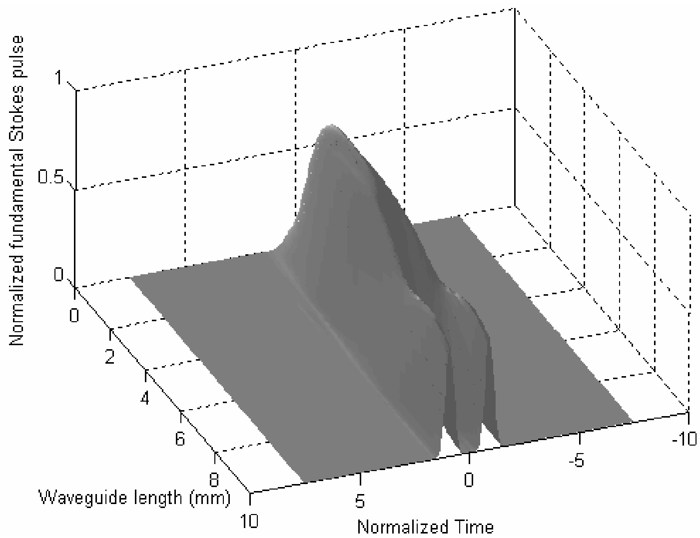

Fig. 3. Evolution of fundamental Stokes pulse in CB section.

The high cancellation rate essentially depends on the relative high level of the Stokes wave at the input of CB, as a result of the amplification process in GB. In Fig. 3 it is visible a depletion effect of the fundamental Stokes wave as induced by the building up of the first order Stokes wave (given in Fig. 4). Then, the waveguide length can be set to $L_2 = 4$ mm in order to avoid the excitation of higher order Stokes waves. Finally, Fig. 5 shows an example of signature operation on the data stream, the cancellation inducing secondary lobes which are 5 dB down with respect to the data pulse.

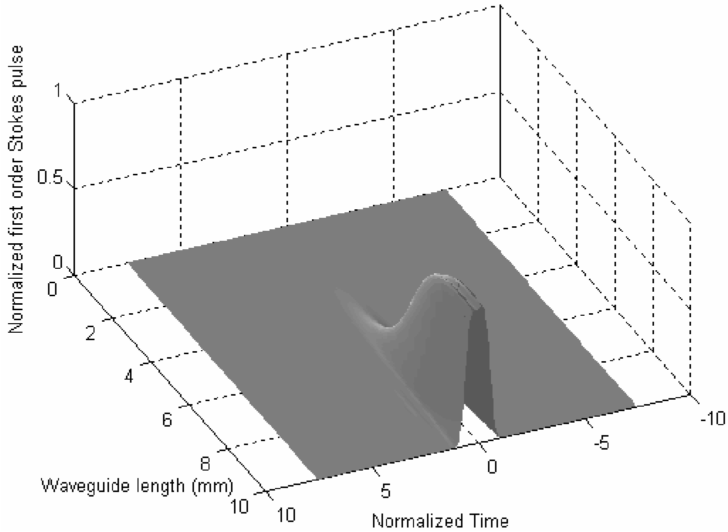

Fig. 4. Space- time evolution of first order Stokes pulse in CB section.

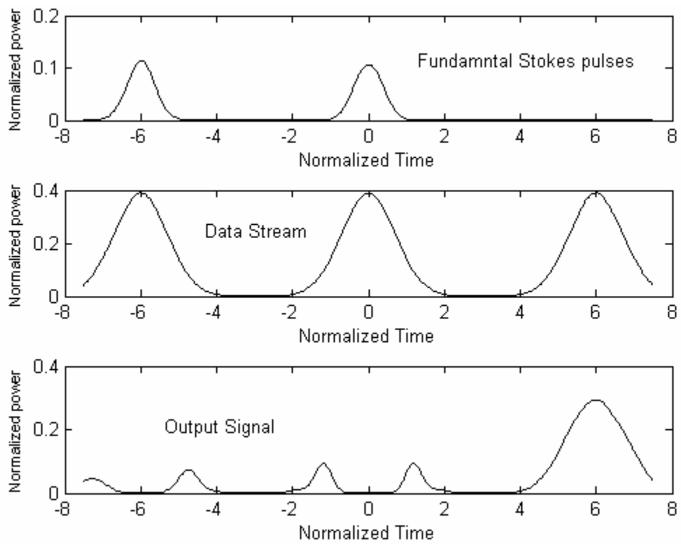

Fig. 5. Interaction between data stream and fundamental Stokes pulses.

Conclusions

In this paper the modelling of a fully integrated optical intensity modulator based on Raman effect in SOI waveguides is presented and discussed. Results are shown as an example of all-optical modulation of a fast data stream.

References

[1] G. Burdge et al., "Ultrafast intensity modulation via Raman gain for all-optical processing," Eur. Conf. on Opt. Commun. Proc., pp. 61-64, 1997.

[2] V.M.N Passaro and F. De Leonardis, "Space-Time Modelling of Raman Pulses in Silicon on Insulator Optical Waveguides", J. Lightwave Technology, vol. 24, pp. 2920-2931, 2006.